A Hybrid Parametrical Wave Prediction Model

H. GUNTHER AND W. ROSENTHAL

Institut fur Geophysik, and Max-Planck-Institut, Hamburg, West Germany

T. J. WEARE AND B. A. WORTHINGTON

Hydraulics Research Station, Wallingford, England

K. HASSELMANN

Max-Planck-Institut, Hamburg, West Germany

J. A. EWING

Institute of Oceanographic Sciences, Wormley, England

The development of a numerical wave prediction model incorporating a parametrical wind-sea model and a characteristic swell model is described. The parametrical model is an extension of an earlier two-parameter model to the full five Jonswap spectral parameters. An application is presented in which the model is used to hindcast severe wave conditions in the North Sea as part of an engineering study to define long-term extreme wave statistics for the area. The limitations of the model and the needs for future research are discussed.

INTRODUCTION

In this paper we describe the continued development of a parametrical wave prediction model. In the Jonswap study (*Hasselmann et al.* [1973]; referred to as I) the overriding importance of nonlinear wave-wave interactions in the dynamics of a growing wind-sea was demonstrated. It was shown that the nonlinear energy transfer controls the rate of growth of the spectrum and furthermore leads to a self-similar spectral shape. A particular spectral parameterization was introduced which fitted closely all the orthogonal fetch limited spectra obtained during Jonswap and in the paper by *Hasselmann et al.* [1976] (referred to as II); it is shown to agree well with data obtained elsewhere under widely differing conditions.

A mathematically rigorous description of the nonlinear interaction is complex, involving as it does the evaluation of the triple Boltzmann integrals. However, a computationally tractable approximation is afforded if the transport equation is projected onto the Jonswap parameter space. A general projection technique is described in I, and a simple two-parameter version of this is given in II. The purpose of the present paper is to extend the wind-sea model developed in II to the full five Jonswap parameters, to incorporate a fully developed sea state, and to include the propagation of swell. The model described herein has a wider application than the early two-parameter model and is expected to be valid for all except the most rapidly varying wind conditions.

SPECTRAL WIND-SEA MODELS: BACKGROUND

A number of wave prediction schemes have been generated during the past two decades. They can be classified broadly into two categories, frequency resolving spectral models and parametrical models. The earliest attempts at wave forecasting, reviewed for instance by *Kinsman* [1965], used significant wave height and wave period and are examples of parametrical models. Early examples of spectral models are those similar to that of *Gelci et al.* [1957], for instance, *Pierson et al.* [1966].

Spectral models, and indeed most modern wave prediction schemes, are based on the energy transport equation, which in deep water has the form

$$\frac{\partial F}{\partial t} + V_i \frac{\partial F}{\partial x_i} = T \tag{1}$$

$F(f, \theta)$ is the wave spectrum energy density, and V_1, V_2 are the components of the wave group velocity for frequency f and direction θ. T is the net source function which regulates the energy budget of the wave field. In general, T contains a generation and a dissipation term. The generation term is composed of a linear growth [*Phillips*, 1957] and an exponential growth [*Miles*, 1957; Phillips, 1966]. The linear growth term is only effective in the early stages of wave growth. The theoretical estimates of the exponential Miles mechanism lead to growth rates an order of magnitude smaller than those actually observed. Therefore the exponential growth coefficient is usually taken from experiment (for example, *Barnett and Wilkerson* [1967] or *Snyder and Cox* [1966] as described by *Inoue* [1967]). The dissipation term can be taken from models of white capping or more usually by empirical functions describing the approach of the spectrum to some fully developed condition.

In the papers of *Phillips* [1960] and *Hasselmann* [1962] the nonlinear interaction of wave trains of different wave number vectors was introduced as a new term in the source function T. The importance of the nonlinear interaction in the development of a wind-sea spectrum has been demonstrated in the Jonswap experiments (I). The addition of this source term to the picture also explains the above-mentioned discrepancy between the measured exponential growth term and that predicted by the theory of Miles-Phillips. In the spectral models of *Barnett* [1968] and *Ewing* [1971] the nonlinear term has been included in a rather simple, parameterized, form. Some method of parameterizing the nonlinear source term is neces-

Paper number 8C0907.
0148-0227/79/008C-0907$01.00

sary, since the exact numerical computations are not feasible within the usual time scale of the model. Once it is admitted that the nonlinear transfers play a dominant role in the energy balance, there is little point in describing the remaining source terms, or the spectrum itself, in greater detail than the parameterized nonlinear term. In the following the methods introduced in I and II will be used to project the energy transport equation (1) onto the five-parameter (Jonswap) space.

THE PARAMETRICAL WIND-SEA MODEL

To transform the transport equation into an equivalent prognostic equation for the spectral parameters, we make the following assumptions concerning the wind-sea wave spectrum.

1. The two-dimensional energy spectrum F has a frequency independent angular distribution Θ, centered on the local wind direction ϕ, i.e.,

$$F(f, \theta) = \Theta(\theta - \phi)E(f) \tag{2}$$

where

$$E(f) = \int F(f, \theta)\, d\theta$$

2. The one-dimensional energy spectrum E can be approximated by the class of functions suggested in I, viz.,

$$\tilde{E}(f) = \alpha g^2(2\pi)^{-4} f^{-5} \exp\left[-\frac{5}{4}\left(\frac{f}{f_m}\right)^{-4} + \ln\gamma \exp\left\{-\frac{(f-f_m)^2}{2\sigma^2 f_m^2}\right\}\right] \tag{3}$$

where

- α Phillips 'constant';
- f_m peak frequency;
- γ peak enhancement factor (= 1 for the Pierson-Moskowitz spectrum);
- σ σ_a for $f \leq f_m$;
- σ_b for $f > f_m$.

Both assumptions depend upon the existence of a dynamic equilibrium between the energy input from the atmosphere and the transfer through wave-wave interactions. In II these assumptions are shown to hold well except when the wind field suffers rapid changes in space or time.

We will further assume that the angular distribution is given by

$$\Theta(\theta - \phi) = \frac{2}{\pi}\cos^2(\theta - \phi) \qquad |\theta - \phi| \leq \pi/2$$

$$\Theta(\theta - \phi) = 0 \qquad \text{otherwise}$$

This form is in broad agreement with the findings of the Jonswap experiments. In any case the model is not critically sensitive to the precise choice of angular distribution. The transport equation (1) can now be integrated over the propagation direction to give

$$\frac{\partial E}{\partial t} + \bar{V}_i \frac{\partial E}{\partial x_i} = S \tag{4}$$

where $\bar{V}$ is the mean group velocity of the one-dimensional spectrum E, i.e.,

$$\bar{V}_i = \frac{\int V_i F d\theta}{E} = \frac{8}{3\pi}\frac{g}{4\pi f}\frac{u_i}{|\mathbf{u}|}$$

where $\mathbf{u}$ is the wind velocity and S equals $\int T d\theta$.

Having removed the angular dependence, the next step is to project the one-dimensional transport equation (4) onto the Jonswap parameter space. The result is (see Appendix A for details) the prognostic equation

$$\frac{\partial a_i}{\partial t} + D_{ijk}\frac{\partial a_j}{\partial x_k} = S_i \qquad k = 1, 2 \qquad i, j = 1, \cdots, 5 \tag{5}$$

where $a_1 = f_m$, $a_2 = \alpha$, $a_3 = \gamma$, and $a_{4,5} = \sigma_{a,b}$. The D_{ijk} matrix is a generalized propagation velocity, the details of which are given in Appendix B.

Turning now to the source function, as was discussed in the above section, three contributions to S can be identified. That is, we may write

$$S = S^{(\text{in})} + S^{(\text{dis})} + S^{(\text{nl})} \tag{6}$$

$S^{(\text{in})}$, $S^{(\text{dis})}$, $S^{(\text{nl})}$ are the mean energy input from the atmosphere, the dissipation of energy, and the nonlinear transfers, respectively. $S^{(\text{dis})}$, includes all energy losses except, of course, the nonlinear transfers. A discussion of these terms is given in I and II.

The general form of the nonlinear source function $S^{(\text{nl})}$ can be deduced to be [*Hasselmann*, 1973]

$$S^{(\text{nl})} \sim \alpha^3 f_m^{-4}\psi(f/f_m) \tag{7}$$

which when projected onto the five-parameter space yields (see Appendix A)

$$S_1^{(\text{nl})} = B_1\alpha^2 f_m^2$$

$$S_2^{(\text{nl})} = B_2\alpha^3 f_m \tag{8}$$

$$S_i^{(\text{nl})} = B_i\alpha^2 f_m \qquad i = 3, 4, 5$$

The coefficients $B_1, \cdots, B_5$ have been determined from computations of the nonlinear source term for the mean Jonswap spectrum (I; *Sell and Hasselmann* [1972]), i.e., for $\gamma \sim 3.3$, $\sigma_a \sim 0.07$ and $\sigma_b \sim 0.09$.

The values obtained are

$$B_1 = -0.54 \qquad B_2 = -5.0 \qquad B_3 = -16.0(\gamma - 3.3)$$

$$B_4 = -[25.5(\sigma_a - 0.07) - 0.5(\sigma_b - 0.09)] \tag{9}$$

$$B_5 = -[25.5(\sigma_b - 0.09) - 0.5(\sigma_a - 0.07)]$$

The coefficient B_1 is not particularly well defined by these calculations. An alternative method is to fix the value of B_1 so as to reproduce the experimentally observed fetch dependence of f_m and α, which we take from II to be

$$f_m = \frac{g}{u}\, 2.84\tilde{x}^{-0.3} \tag{10a}$$

and

$$\alpha = 0.0662\tilde{x}^{-0.2} \tag{10b}$$

where $\tilde{x} = gx/u^2$, x is fetch, and u is wind speed at 10 m above sea surface.

Substituting (10) into (5) for $i = 1$ yields a value of $B_1 = -0.586$, which is agreeably close to the theoretical estimate. This value of B_1 is the one used in the model.

For the remainder of the source term we assume the minimal dissipation case discussed in I. That is, in the frequency range we are dealing with ($f \leq 0.7$ Hz), dissipation is neglected. This leaves just the input source term for which we assume the spectral dependence predicted by the Miles generation mechanism, i.e.,

$$S^{(\text{in})} = \beta(f)E(f) \tag{11}$$

Projecting $S^{(in)}$ onto the spectral parameter space leads to only one nonzero source function, viz.,

$$S_2^{(in)} = \alpha f_m g(\nu) \tag{12}$$

where

$$\nu = f_m u/g$$

The function $g(\nu)$ can be determined from the fetch-limited behavior of f_m and α, i.e., from (5) and (10), with the result

$$S_2^{(in)} = 5.022 \times 10^{-3}\nu^{4/3}\alpha f_m \tag{13}$$

Finally, to complete our description of the wind-sea parametrical model, we need to incorporate a transition to the fully developed sea (PM) [*Pierson and Moskowitz*, 1964]. The spectral parameters α and f_m have fixed values for the PM spectrum, namely, $\alpha = 0.0081$ and

$$f_m = \left(\frac{0.74}{1.25}\right)^{1/4} \frac{g}{2\pi U_{19.5}} = 0.13\,\frac{g}{u} \tag{14}$$

Note that allowance has to be made for the differing choice of anemometer heights (19.5 m in the Pierson-Moskowitz study and 10 m in the present case [*Pierson*, 1977]).

With the peak enhancement factor $\gamma = 1$ the Jonswap spectral form then reduces to the PM spectrum. Thus transition to the PM fully developed sea requires $\alpha \to 0.0081$ and $\gamma \to 1$ as $\nu \to 0.13$. Also, of course, the source terms vanish, i.e., $S_i \to 0$. This is achieved by modifying the source functions as follows:

$$\begin{aligned}
S_1 &= -0.586\alpha^2 f_m{}^2 \left(\frac{\gamma - 1}{2.3}\right) \quad \nu > 0.13 \\
S_1 &= 0 \quad \text{otherwise} \\
S_2 &= (5.022 \times 10^{-3}\nu^{4/3} - 5\alpha^2)\alpha f_m \\
S_3 &= -16.0(\gamma - \gamma_0)\alpha^2 f_m \\
S_4 &= -[25.5(\sigma_a - 0.07h) - 0.5(\sigma_b - 0.09h)]\alpha^2 f_m \\
S_5 &= -[25.5(\sigma_b - 0.09h) - 0.5(\sigma_a - 0.07h)]\alpha^2 f_m
\end{aligned} \tag{15}$$

where

$$\begin{aligned}
\gamma_0 &= 3.3 \quad \nu \geq 0.16 \\
\gamma_0 &= 1 + 2.3\,\frac{\nu - 0.13}{0.03} \quad 0.16 > \nu > 0.13 \\
\gamma_0 &= 1 \quad 0.13 \geq \nu
\end{aligned}$$

and

$$h = \left(\frac{4.0}{\gamma + 0.7}\right)^2$$

The modified source functions given in (15) produce the desired transition from the growing sea to the fully developed sea in the frequency range $0.13 \leq \nu \leq 0.16$.

THE SWELL MODEL

The parametrical model described above is only valid in the wind-sea region of the energy spectrum, that is, for wind speeds such that $\nu \geq 0.13$. For wind speeds below that corresponding to $\nu = 0.13$, i.e., for $u < g(0.13/f_m)$, the phase velocity of the waves exceeds the wind speed, and it is assumed that no energy is absorbed from the atmosphere. Thus the energy spectrum cannot be maintained at a level at which the nonlinear wave-wave interactions are effective and the wave

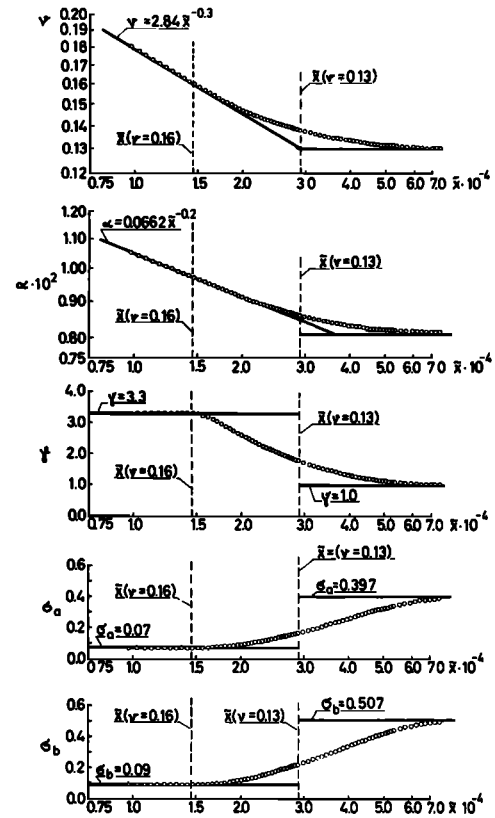

Fig. 1. The modelled fetch dependence of the wind-sea parameters, shown by circles. $\tilde{x} = gx/u^2$ is the nondimensional fetch (x is fetch, g is gravitational constant, and u is wind speed).

field propagates freely as swell (if bottom dissipation is ignored). The problem therefore reduces to solving the transport equation (1) without a source function input (i.e., $T = 0$). This can be handled by one of two methods. The transport equation can be modelled by using a finite difference scheme, i.e., (1) is discretized on a space-time grid and the various derivatives are approximated by finite differences. This approach has the advantage that the swell field can be represented on the same space-time grid as the wind-sea parameters. It has the disadvantage of requiring the use of high-order finite difference schemes to control the effects of numerical dispersion which would otherwise seriously distort the swell field as it propagates. In addition, a finite difference representation of the transport equation does not extend very easily to the inclusion of refraction effects.

The alternative is to represent the swell field on a set of characteristics (rays). That is, for each swell frequency f required, the model is covered with a mesh of rays at appropriate angles and spacing (curvature due to refraction being included if necessary). A similar technique has been used by *Barnett et al.* [1969]. Swell is represented as discrete energy packets at points spaced along each ray at intervals of $\Delta l = \Delta t v$, where Δt is the model time step and v is the group velocity at frequency f ($= g/4\pi f$ in deep water). If the ray points are stored in a one-dimensional string, propagation by one or more time steps is a simple array or input-output process. There remains, of course, the problem of transforming back and forth between the ray characteristics and the cartesian wind-sea grid. However, provided the spatial density of the ray points is comparable with that of the wind-sea grid (and indeed there is little point in describing the swell field to a greater

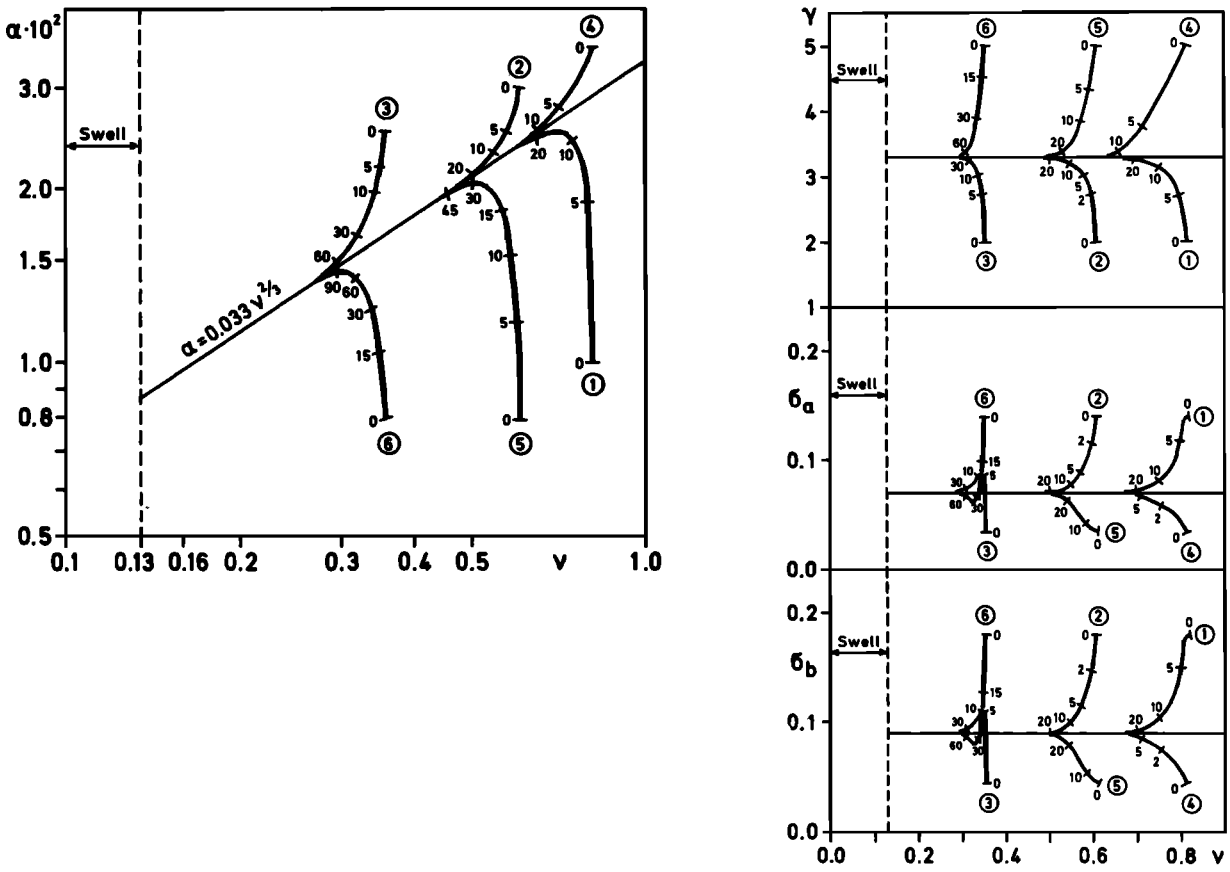

Fig. 2. Relaxation of the five model parameters to equilibrium. The initial values for the six runs shown are given in Table 1. The numbers along the curves give the elapsed time in minutes.

resolution than the wind-sea), the transformations can be treated as a more or less one to one correspondence. In the application described in the following the characteristic method has been adopted.

THE HYBRID WIND-SEA/SWELL MODEL

To combine the parametrical wind-sea model and the swell model, we have to establish dynamical criteria to decide when energy is to be transferred between the two domains of the wave spectrum. The implications of the existing theories of nonlinear interactions and atmospheric input have not yet been fully explored and so it is necessary to formulate our exchange criteria on intuitive grounds. In doing so, two principles have been observed. First, it is assumed that the total energy (wind-sea + swell) is conserved in any exchange. Second, the nonlinear interaction between swell and wind-sea is very weak unless the swell and wind-sea frequency domains overlap. When overlap occurs, the interaction is such that the coupling or decoupling of the two is rapid (i.e., within a model time step). Support for this point of view can be found in the computations of *Hasselmann* [1963].

TABLE 1. Initial Values for the Grid Points in Runs 1–6 of Figure 2

	Run 1	Run 2	Run 3	Run 4	Run 5	Run 6
f_m, s^{-1}	0.8	0.6	0.35	0.8	0.6	0.35
α	0.01	0.03	0.025	0.035	0.008	0.008
γ	2.0	2.0	2.0	5.0	5.0	5.0
σ_a	0.14	0.14	0.035	0.035	0.035	0.14
σ_b	0.18	0.18	0.045	0.045	0.045	0.18

The following criteria have been adopted for wind-sea to swell transfers, when the peak frequency f_m falls below the peak frequency of a fully developed sea f_{PM}, i.e., when

$$f_m < \frac{0.13g}{u} = f_{PM} \tag{16}$$

1. f_m is set to f_{PM}.
2. α is adjusted to a new value α' such that the spectral energy for frequencies above f_{PM} is conserved in the wind-sea, i.e.,

$$\int_{f_{PM}}^{\infty} E_{ws}(\alpha, f_m, \gamma)\, df = \int_{f_{PM}}^{\infty} E_{ws}(\alpha', f_{PM}, \gamma = 1)\, df \tag{17}$$

where E_{ws} denotes the parametrical wind-sea spectrum as given in (3).

3. Overall energy conservation is achieved by transferring to swell the wind-sea spectrum for $f < f_c$, where the cutoff frequency f_c is defined so that the total energy in the remaining wind-sea spectrum is equal to the energy in the original wind-sea spectrum for $f > f_c$, i.e.,

$$\int_{f_c}^{\infty} E_{ws}(\alpha, f_m, \gamma)\, df = \int_{0}^{\infty} E_{ws}(\alpha', f_{PM}, \gamma)\, df \tag{18}$$

Because the integrals in (17) and (18) cannot be expressed analytically (except when $\gamma = 1$), it is necessary to evaluate α' and f_c numerically. The wind-sea energy transferred to swell is distributed with a $\cos^2$ spreading function.

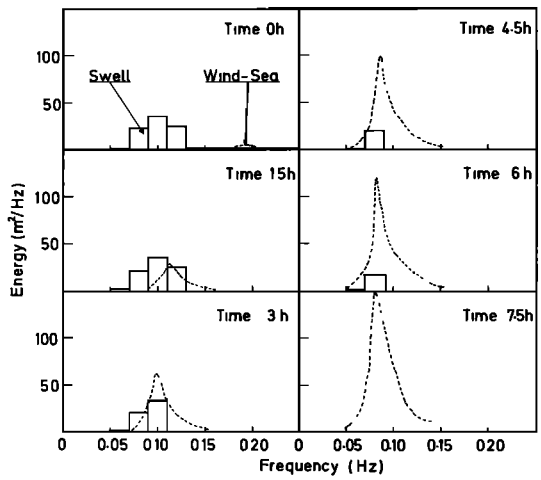

Fig. 3. Modeled growth of duration-limited wind-sea when swell energy exists. A constant wind of 20 m/s is blowing.

The reverse exchange of swell to wind-sea is called into play whenever swell energy is found at a frequency greater than $0.9f_m$, where f_m as usual is the frequency of the wind-sea peak. The swell within this frequency range is assumed to be instantaneously absorbed (i.e., within one model time step) into the wind-sea irrespective of direction. Energy is conserved by adjusting the frequency of the wind-sea peak from f_m to f_m', keeping α and γ fixed, i.e.,

$$\delta E_{\text{swell}} + \int_0^\infty E_{ws}(\alpha, f_m, \gamma)\, df = \int_0^\infty E_{ws}(\alpha, f_m', \gamma)\, df \qquad (19)$$

where δE_{swell} is the total swell energy transferred. Again, the integrals involved generally cannot be expressed analytically. However, they are readily approximated numerically as tabulated functions of γ.

To conclude this discussion of wind-sea and swell exchange, a further eventuality must be considered. Situations will arise in which energy exists in the swell domain at frequencies outside the range of the wind-sea nonlinear interaction (i.e., $f < 0.9f_m$) but within the influence of the atmospheric input, i.e., $f > f_0 = g/2\pi u \cos\theta$, where θ is the angle between the swell direction and the wind velocity vector. Thus swell in the range $f_0 < f < 0.9f_m$ is assumed to grow through the Miles-Phillips mechanism with a source function given by [*Snyder*, 1974]

$$S(f, \theta) = \beta(f, \theta)F(f, \theta) \qquad (20)$$

where

$$\beta = 2\pi f \left(\frac{f}{f_0} - 1\right) \frac{\rho_a}{\rho_w} c \qquad f > f_0$$

$$\beta = 0 \qquad f \le f_0$$

F is the swell energy density, ρ_a, ρ_w is the density of air, water, and c is a constant taken as 0.05.

The wind-sea model and the swell model together with the exchange criteria outlined above constitute the hybrid wave model.

Detailed accounts of the numerical and computational techniques employed in implementing the hybrid model can be found in *Hydraulics Research Station* [1977*a*, *b*]. A brief outline of some of the more important aspects is given by *Ewing et al.* [1979].

Application to Idealized Situations

In order to demonstrate that the model describes the development of the wind-sea parameters (f_m, α, γ, σ_a, σ_b) correctly, it is applied to simple idealized situations.

Figure 1 shows the modelled behavior of the five wind-sea parameters under fetch-limited conditions. In the case shown the wind velocity is 5 m/s blowing orthogonally offshore. The parameters f_m and α obey the prescribed fetch laws (10) and adjust at large fetch to their Pierson-Moskowitz limiting values. The shape parameters γ, σ_a, σ_b stay at their statistical means for the developing sea and adjust for large fetches to reproduce the fully developed sea state.

For the small range of ν ($f_m u/g$) in which the wave spectrum is expected to approach the Pierson-Moskowitz form, the source functions are adjusted as defined in (15) to achieve a smooth transition from the solution for a growing wind-sea to that of the fully developed sea state. The extent of this transition range, although not critical for practical purposes, is not well defined in terms of the presently available wave data.

Other comparison of numerical results for simple wind situations (for which analytical solutions of the two-parameter model are given in II) can be found in the work of *Günther and Rosenthal* [1976].

Figure 2 shows the relaxation of the wind-sea parameters after an initial displacement from their equilibrium curves. In equilibrium, fetch-limited conditions exist with a wind of 10 m/s blowing orthogonally offshore. An integration time step of 60 s and a grid spacing of 2000 m are used. There are 23 grid points along the wind direction, the first point, 5000 m from the shore, having fixed boundary conditions.

Six runs are presented with the spatially constant initial values given in Table 1. The results are plotted for the eleventh grid point.

The straight lines in the figures show the equilibrium lines of α, $\nu = uf_m/g$ and the average values of the shape parameters, respectively. The numbers by the curves give the integration time in minutes.

The examples show that ν and α behave as in the two-parameter model (II).

The evolution of γ, σ_a, σ_b shows a relaxation time to return to their statistical mean which is of the same order as the time taken by ν and α to return to their equilibrium curve.

This return to equilibrium is governed by the stabilizing nonlinear transfer and is an order of magnitude more rapid than the rate of migration of the peak frequency along the equilibrium line once equilibrium has been established.

Figure 3 shows the growth of duration-limited wind-sea under the action of a constant wind of 20 m/s when swell energy exists. An integration time step of 1½ hours is used.

The wind-sea absorbs the swell and grows at a faster rate than it would without the swell. The rate of growth of total energy however (inclusive of swell) is similar to what would have occurred if all the original energy were in the wind-sea.

Norswam Project

The sharp increase of engineering activity in the North Sea in recent years has generated a need for reliable long-term extreme wave statistics to assist in the design of offshore structures. In view of the long period and high cost involved in gathering wave measurements, a numerical model offers the only method of establishing a statistically valid data base. For this reason the Norswam model was developed to hindcast wave conditions from a retrospective analysis of the wind field

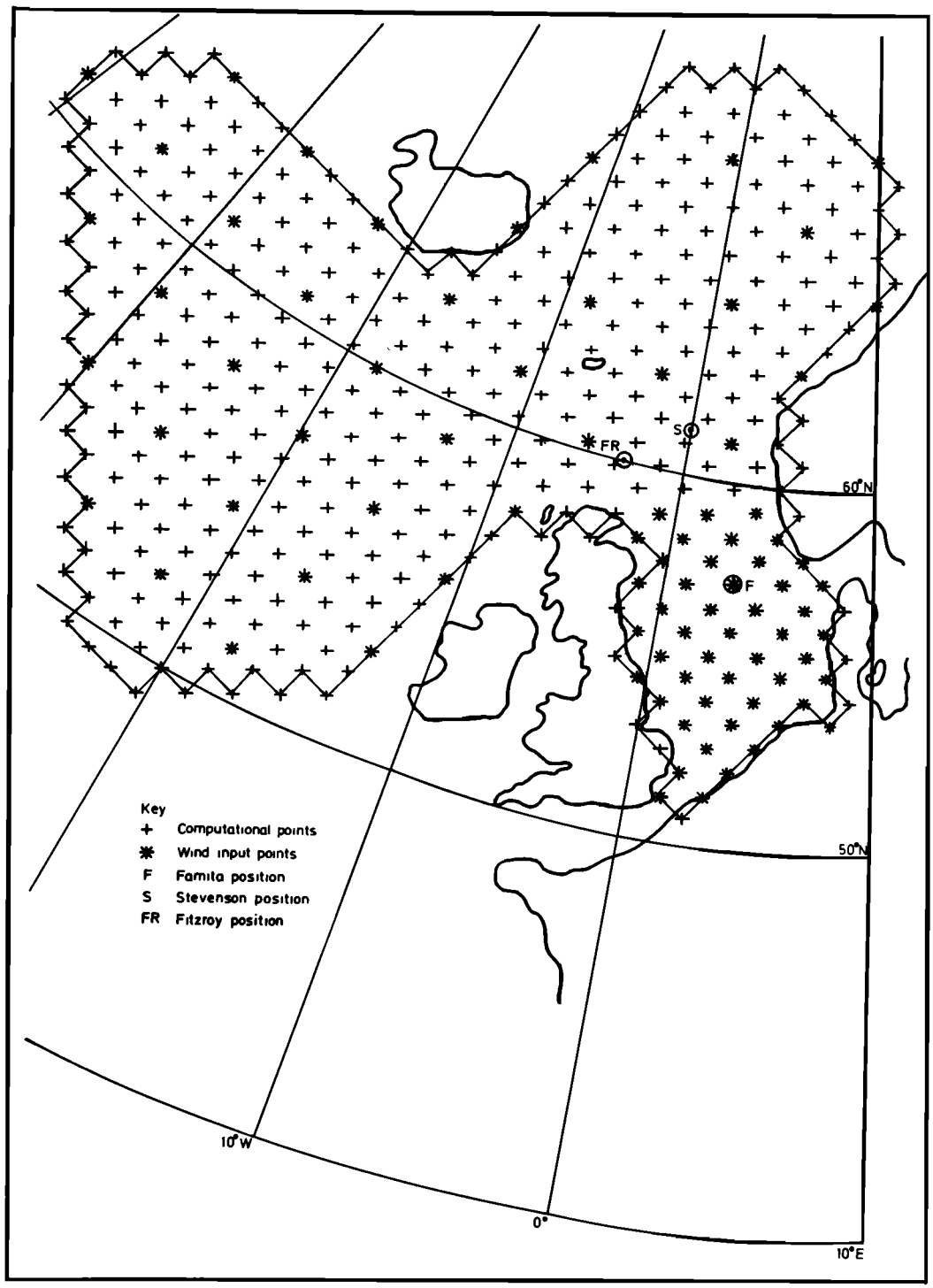

Fig. 4. Grid used in the numerical wave model. The wind field is defined on a 100-km grid within the North Sea and a 300-km grid elsewhere. Wave computations are made on the 100-km grid over the whole area. Wave measurements have been made at stations Famita, Fitzroy, and Stevenson.

for a number of severe storms representing the decade 1966–1976. The project has been jointly financed by the UK Departments of Energy and Industry, the Hydraulics Research Station (UK), and the UK Offshore Operators Association. The collaborating German group is supported by the Deutsche Forschungsgemeinschaft, Sonderforschungsbereich 94 at the University of Hamburg.

The model grid selected for the wave calculations is shown in Figure 4. It is part of the grid used by the UK Meteorological Office atmospheric model. Based on a stereographic projection, it has an average grid spacing of 100 km. The model boundaries extend well to the north and west of the area of primary interest, the northern North Sea.

The analysis of the wind field was carried out [*Harding and Binding*, 1978] by the Institute of Oceanographic Sciences (UK). From a total of more than 200 gale occurrences during the period 1966–1976 a subset of 42 severe storms was selected for analysis. As far as possible, the relative occurrence of

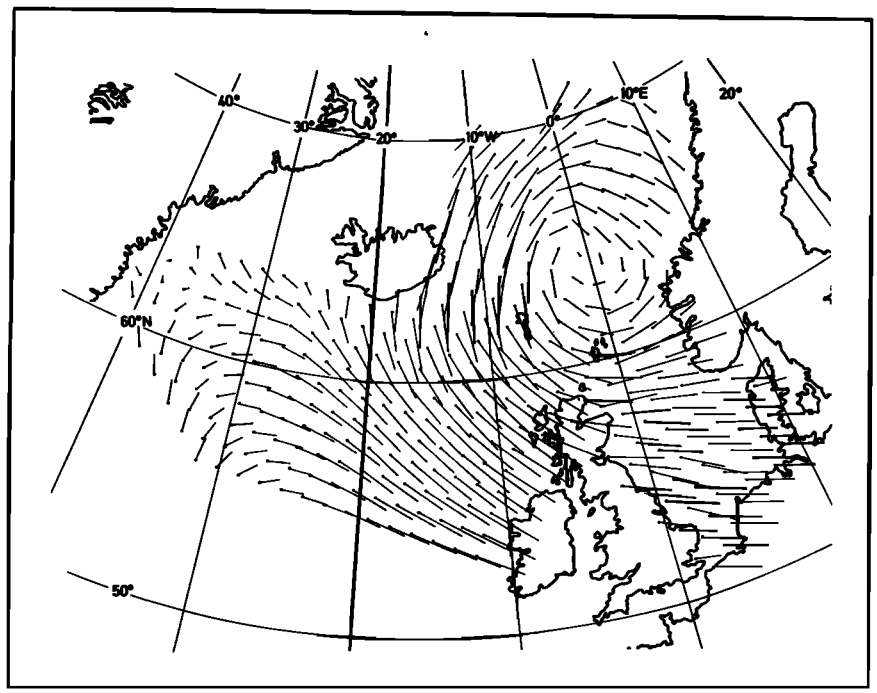

Fig. 5. Example of the wind field input to the numerical model. The vectors show strength and direction of the wind.

storms according to type and monthly/annual frequency was preserved in the selection. Synoptic weather charts were reanalyzed to incorporate late ship reports and oil-rig observations. Corrections were made for atmospheric stability and for markedly cyclonic flows. The wind field is specified every 3 hours throughout each storm at the grid points indicated in Figure 3. Linear interpolation in space and time provides values on the 100-km grid and 1½-hour integration step required by the model. An example of the wind field input for one time step is shown in Figure 5.

In the hybrid wave model used in this study only the f_m, α, and γ parameters were treated as free, the peak width parameters being fixed at their mean Jonswap values of $\sigma_a = 0.07$ and $\sigma_b = 0.09$.

Calibration of the model was achieved by comparison with wave recorder data for 15 storms at two sites (see Figure 3 for locations). It is clear that there is some latitude in fixing the atmospheric input source term $S_2^{(\mathrm{in})}$ by reference to the fetch dependence of α and f_m observed in the Jonswap experiment. Therefore the source function was not assumed to be fixed as given in (13) but was parameterized as

$$S_2^{(\mathrm{in})} = a\nu^p \alpha f_m \tag{21}$$

Various combinations of the values of the coefficient a and exponent p were tested, and the model and observed values for the significant wave height H_s and mean zero upcrossing period T_z compared, where

$$H_s = 4.0 m_0^{1/2} \quad T_z = (m_0/m_2)^{1/2} \quad m_n = \int_0^\infty f^n E(f) df$$

Values of $a = 5.12 \times 10^{-3}$ and $p = 1.314$ were found to minimize the bias in H_s at the Famita and Stevenson weathership positions (see Figure 3). These values are very close to those deduced from the Jonswap data in (13).

Comparisons of model and measured H_s, T_z and wave

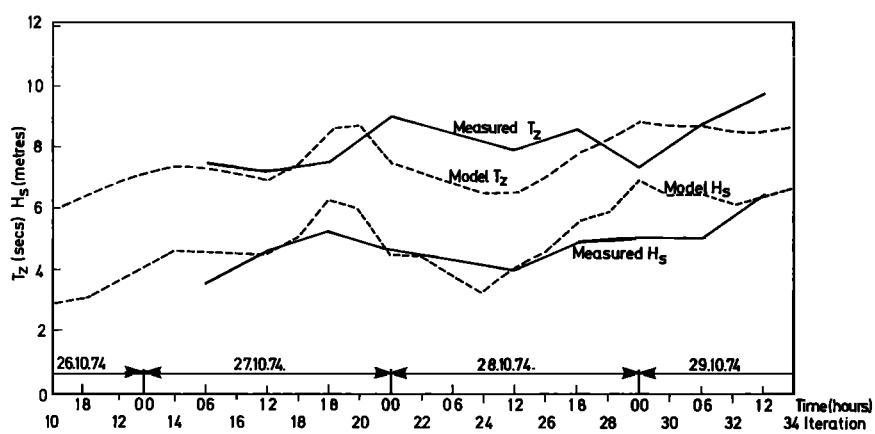

Fig. 6. Comparison of measured (solid line) and hindcast (dashed line) significant wave height and zero-crossing period at station Famita for the storm of October 26–29, 1974.

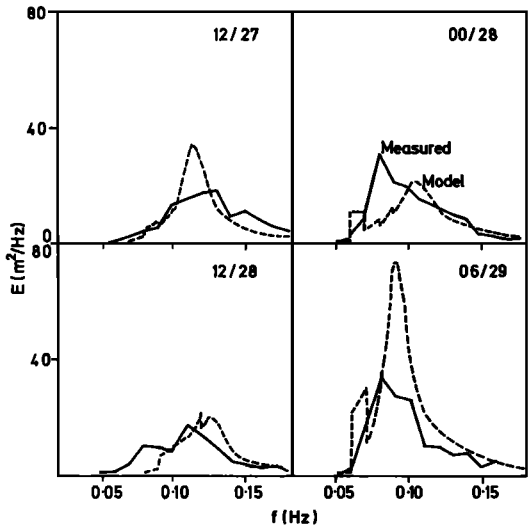

Fig. 7. Comparison of measured (solid line) and hindcast (dashed line) wave spectra at station Famita for the storm of October 26–29, 1974.

spectra for the storms of October 26–29, 1974, and December 17–18, 1974, at the Famita weathership position (57°30N, 3°00′E) are presented in Figures 6–9. The measured spectra were obtained from a shipborne wave record by a fast Fourier transform method.

To determine whether the inaccuracy of the model for some storms is due to the rather coarse (eight directions) swell definition, a test run was made for one storm (October 26–29, 1974) with swell rays defined every 30° rather than 45°. Very little difference occurred, indicating that the 45° spacing is adequate. The resolution provided by such a coarse spacing is probably sufficient, since the model is here being applied to extreme wave conditions and thus swell in the model is generally used for temporary dumping of wind-sea energy during the passage of a depression and is rapidly absorbed when the wind rises.

The correlation between model results and measured wave data can be summarized for the Famita and Stevenson positions by a straight line fit by regression analysis, weighting each point according to storm distribution and relative abundance of data for that storm's class.

For predicted and observed maxima of H_s the fit is

$$H_{s_{\text{measured}}} = 0.985 H_{s_{\text{model}}}$$

with a standard error of 0.7 m, or 10% of the mean.

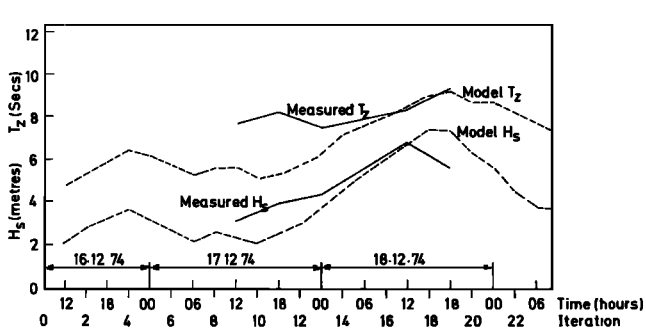

Fig. 8. Comparison of measured (solid line) and hindcast (dashed line) significant wave height and zero-crossing period at station Famita for the storm of December 17–18, 1974.

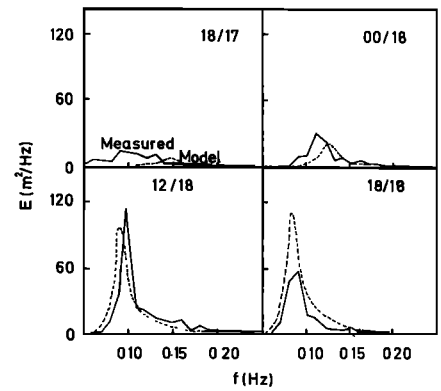

Fig. 9. Comparison of measured (solid line) and hindcast (dashed line) wave spectra at station Famita for the storm of December 17–18, 1974.

When all of the observed data, that is, not just the storm maxima, are taken into account, the fit becomes

$$H_{s_{\text{measured}}} = 1.010 H_{s_{\text{model}}}$$

with standard error 1.4 m, or 25% of the mean.

Further details of these and other comparisons can be found in *Hydraulics Research Station* [1977*a*].

Many different causes contribute to the above scatter, e.g., errors in the wave measurements or a breakdown in the theoretical assumptions underlying the model. But probably the most important effects stem from errors in the wind field input and from the inherent small-scale variability in the wave field. To estimate the size of the errors involved in the wind analysis, the model input wind speed has been compared with reported winds at the weathership Fitzroy (60°00′N, 4°00′W) (see Figure 10). These observations were not incorporated in the original analysis of the wind field and therefore constitute an independent check. The scatter has a standard deviation of 24% of the mean (based on 110 points) with a bias of about 6%. Since the wind speed and significant wave height H_s are more or less

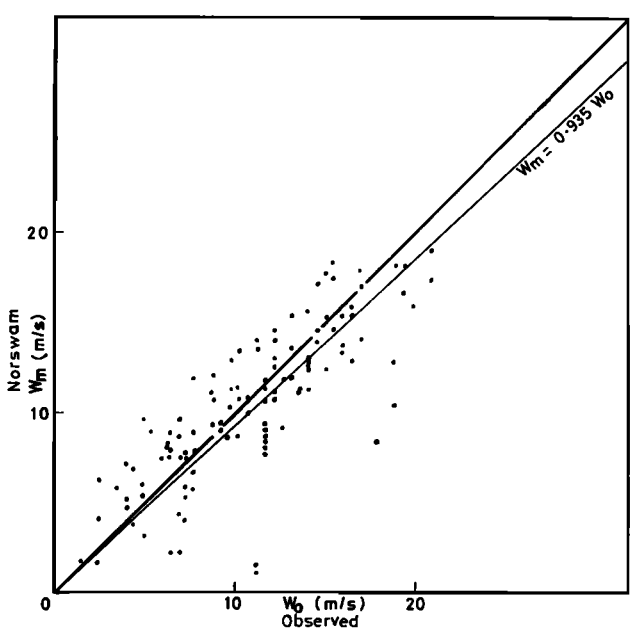

Fig. 10. Comparison of reported winds with model input winds at station Fitzroy for storm of winter 1974/1975.

linearly related for fetch and duration limited conditions, a scatter of a similar magnitude is expected in H_s.

In addition to the input 'noise' due to the limitations of the meteorological information, there is an inherent variability in the wave field stemming from small-scale gustiness in the wind (see I and II for further discussion of this point). In II it is shown that the scale parameters α and f_m obtained from a large number of field studies group around a universal curve in the α-ν plane, a fact which receives a natural explanation in terms of a dynamic balance between the atmospheric input and the nonlinear transfers. However, there is a scatter of about 38% about this equilibrium curve (see II, data set *J*). If the variability in α is due to a small-scale variability in the wave field, then we would expect a scatter in the comparison of the model and measured H_s values of about 19% due to this cause alone ($H_s \sim \alpha^{1/2}$). The overall agreement between the model predictions and wave recorder data is therefore reasonable, and long-term wave statistics have been deduced from the model output [*Ewing et al.*, 1979].

CONCLUSIONS

The development of the parametrical wave prediction model started by *Hasselmann et al.* [1973, 1976] has been taken a stage further with the inclusion of swell and of a transition to a fully developed sea. The model in its present form should have a wide applicability. The parametrical description of the wind-sea which has been pursued here constitutes a practical compromise in which only the essential physical processes which govern the evolution of the spectrum are modelled. In this way an economically feasible model has been achieved.

A number of limitations have been identified, some of a fundamental nature and others which we fully expect will be removed in the next phase of development. The inherent variability in the wave field sets a fundamental limit to the accuracy of model predictions, as does the reliability of the input wind field. Areas deserving further research concern the wind-sea to swell transitions, the approach to a fully developed state, and the assumption of a fixed angular distribution tied to the local wind direction. A more detailed study of the nonlinear source term is planned and promises to shed light on these problems. The aim is to extend the model so that rapidly varying winds can be accommodated, enabling extreme situations, such as a hurricane or waves generated under severely restricted fetch conditions, to be handled by the model.

APPENDIX A. FUNCTIONALS FOR WIND SEA PARAMETERS AND THEIR FUNCTIONAL DERIVATIVES

The technique for optimally fitting the wind-sea parameters to a spectrum which defines the parameter functionals is given by *Müller* [1976]. For our purposes, however, we redefine some of the functionals slightly for computational simplicity.

TABLE B1. The Coefficients D_{ij} as They Emerge From (B1)

	j		
i	1	2	3
1	$v\cdot(1 + 5K)$	$-v\frac{f_m}{\alpha}K$	$-v\frac{f_m}{\gamma}K$
2	$-v\frac{\alpha}{f_m}0.4588$ $+\frac{\alpha}{f_m}0.7216D_{11}$	$v\cdot 0.6047$ $+\frac{\alpha}{f_m}0.7216D_{12}$	$\frac{\alpha}{f_m}0.7216D_{13}$
3	$-v\frac{\gamma}{f_m}\cdot 5 + \frac{\gamma}{f_m}5D_{11}$ $-\frac{\gamma}{\alpha}D_{21}$	$v\frac{\gamma}{\alpha} + \frac{\gamma}{f_m}5D_{12}$ $-\frac{\gamma}{\alpha}D_{22}$	$v + \frac{\gamma}{f_m}5D_{13}$ $-\frac{\gamma}{\alpha}D_{23}$
4	$\frac{1-\sigma_a}{f_m}D_{11} + \frac{e^{1/2}}{\ln\gamma}\sigma_a\left\{-v\frac{1}{f_m}\left[5(1-\sigma_a)^{-5} + \frac{\ln\gamma}{\sigma_a}e^{-1/2}\right] + \frac{5}{f_m}(1-\sigma_a)^{-4}D_{11} - \frac{1}{\alpha}D_{21} - \frac{e^{-1/2}}{\gamma}D_{31}\right\}$	$\frac{1-\sigma_a}{f_m}D_{12} + \frac{e^{1/2}}{\ln\gamma}\sigma_a\left\{v\cdot\frac{1}{\alpha}(1-\sigma_a)^{-1} + \frac{5}{f_m}(1-\sigma_a)^{-4}D_{12} - \frac{1}{\alpha}D_{22} - \frac{e^{-1/2}}{\gamma}D_{32}\right\}$	$\frac{1-\sigma_a}{f_m}D_{13} + \frac{e^{1/2}}{\ln\gamma}\sigma_a\left\{v\cdot\frac{e^{-1/2}}{\gamma}(1-\sigma_a)^{-1} + \frac{5}{f_m}(1-\sigma_a)^{-4}D_{13} + \frac{1}{\alpha}D_{23} - \frac{e^{-1/2}}{\gamma}D_{33}\right\}$
5	$-\frac{1+\sigma_b}{f_m}D_{11} + \frac{e^{1/2}}{\ln\gamma}\sigma_b\left\{-v\frac{1}{f_m}\left[5(1+\sigma_b)^{-5} - \frac{\ln\gamma}{\sigma_b}e^{-1/2}\right] + \frac{5}{f_m}(1+\sigma_b)^{-4}D_{11} - \frac{1}{\alpha}D_{21}\frac{e^{-1/2}}{\gamma}D_{31}\right\}$	$-\frac{1+\sigma_b}{f_m}D_{12} + \frac{e^{1/2}}{\ln\gamma}\sigma_b\left\{v\cdot\frac{1}{\alpha}(1+\sigma_b)^{-1} + \frac{5}{f_m}(1+\sigma_b)^{-4}D_{12} - \frac{1}{\alpha}D_{22} - \frac{e^{-1/2}}{\gamma}D_{32}\right\}$	$-\frac{1+\sigma_b}{f_m}D_{13} + \frac{e^{1/2}}{\ln\gamma}\sigma_b\left\{v\cdot\frac{e^{-1/2}}{\gamma}(1+\sigma_b)^{-1} + \frac{5}{f_m}(1+\sigma_b)^{-4}D_{13} - \frac{1}{\alpha}D_{23} - \frac{e^{-1/2}}{\gamma}D_{33}\right\}$

All coefficients not shown are zero.
$D_{44} = v(1-\sigma_a)^{-1}$, $D_{55} = v(1+\sigma_b)^{-1}$, $v = g/4\pi f_m$, $K = \sigma^2/(20\sigma^2 + \ln\gamma)$, and $\sigma = \frac{1}{2}(\sigma_a + \sigma_b)$.

TABLE B2. The Coefficients D_{ij}, Modified to Prevent Singularities Caused by Special σ Values

i	j = 1	j = 2	j = 3
1	$v(1 + 5K)$	$-v\frac{f_m}{\alpha}K$	$-v\frac{f_m}{\gamma}K$
2	$v\frac{\alpha}{f_m}(0.2628 + 3.608K)$	$v(0.6047 - 0.7216K)$	$-v\frac{\alpha}{\gamma}0.7216K$
3	$-v\frac{\gamma}{f_m}(0.2628 - 21.392K)$	$v\frac{\gamma}{\alpha}(0.3953 - 4.2784K)$	$v(1 - 4.2784K)$
4	$-v\frac{1}{f_m}\{5K(\sigma_a - 1) + \sigma_a + \frac{\sigma_a}{\ln\gamma}[8.2436\sigma_a + 0.17048 - K(164.87\sigma_a + 13.877]\}$	$v\frac{1}{\alpha}\{K(\sigma_a - 1) + \frac{\sigma_a}{\ln\gamma}[-K(2.7755 + 32.974\sigma_a) + 1.6487\sigma_a + 0.25644]\}$	$v\frac{1}{\gamma}\{K(\sigma_a - 1) + \frac{\sigma_a}{\ln\gamma}[\sigma_a - K(32.974\sigma_a + 2.7755)]\}$
5	$v\frac{1}{f_m}\{-5K(1 + \sigma_b) - \sigma_b + \frac{\sigma_b}{\ln\gamma}[8.2436\sigma_b - 0.17048 - K(164.87\sigma_b - 13.877)]\}$	$-v\frac{1}{\alpha}\{-K(1 + \sigma_b) + \frac{\sigma_b}{\ln\gamma}[-K(-2.7755 + 32.974\sigma_b) + 1.6487\sigma_b - 0.25644]\}$	$-v\frac{1}{\gamma}\{-K(1 + \sigma_b) + \frac{\sigma_b}{\ln\gamma}[\sigma_b - K(32.974\sigma_b - 2.7755)]\}$

$D_{44} = v(1 + \sigma_a)$, $D_{55} = v(1 - \sigma_b)$, $v = g/4\pi f_m$, $K = \sigma^2/(20\sigma^2 + \ln)$, and $\sigma = \frac{1}{2}(\sigma_a + \sigma_b)$.

In the first part of this appendix we list the functionals we have chosen; in the second we give the functional derivatives that are used to project the prognostic equation (4) into the parameter space.

The peak frequency f_m of a one-dimensional spectrum $E(f)$ is defined as the solution of the equation

$$E'(f) = \frac{\partial E(f)}{\partial f} = 0 \tag{A1}$$

To give our functional a more tractable form, we write

$$a_1 = f_m = \phi_1(E) = \int f\delta(E'(f))d(E'(f)) \tag{A2}$$

The parameter $a_2 = \alpha$ is defined by

$$a_2 = \alpha = \phi_2(E) = \frac{1}{0.65 f_m} \cdot \int_{1.35 f_m}^{2 f_m} \frac{E(f)f^5}{g^2(2\pi)^{-4}} \exp\left[\frac{5}{4}\left(\frac{f}{f_m}\right)^{-4}\right] df \tag{A3}$$

For the parameter γ we first form the Pierson-Moskowitz spectrum according to the above defined parameters f_m, α:

$$E_{PM} = \alpha g^2(2\pi)^{-4} f^{-5} \exp\left[-\frac{5}{4}\left(\frac{f}{f_m}\right)^{-4}\right] \tag{A4}$$

and find γ by

$$a_3 = \gamma = \phi_3(E) = \int \frac{E(f)}{E_{PM}(f)}\delta(f - f_m)df \tag{A5}$$

To define the remaining functionals, we use the function

$$g(f) = \ln\frac{E(f)}{E_{PM}(f)} - e^{-0.5}\ln\gamma \tag{A6}$$

The zeros of $g(f)$ are

$$h_a = f_m(1 - \sigma_a) \qquad h_b = f_m(1 + \sigma_b) \tag{A7}$$

Therefore we get

$$a_4 = \sigma_a = 1 - \frac{1}{f_m}\int_{f<f_m} f\delta(g(f))d(g(f)) \tag{A8}$$

$$a_5 = \sigma_b = -1 + \frac{1}{f_m}\int_{f>f_m} f\delta(g(f))d(g(f)) \tag{A9}$$

The functional derivatives ϕ_j' are defined by

$$\delta a_j = \phi_j'(\delta F) \tag{A10}$$

These follow from (A2), (A3), (A5), (A8), and (A9) as

$$\phi_1'(G(f)) = -\frac{1}{E''(f_m)}\int \delta(f - f_m)\frac{d}{df}[G(f)]\,df \tag{A11}$$

$$\phi_2'(G(f)) = \frac{\alpha}{0.65 f_m}\int_{1.35 f_m}^{2 f_m}\frac{1}{E_{PM}(f)}[G(f)]\,df + \frac{\alpha}{f_m}0.722\phi_1'(G(f)) \tag{A12}$$

$$\phi_3'(G(f)) = \int \delta(f - f_m)\frac{1}{E_{PM}(f)}[G(f)]\,df + \gamma\left[\frac{5}{f_m}\phi_1'(G(f)) - \frac{1}{\alpha}\phi_2'(G(f))\right] \tag{A13}$$

$$\phi_4'(G(f)) = \frac{1}{f_m}\left[\frac{h_a}{f_m}\phi_1'(G(f)) + \frac{1}{g'(h_a)}\left(\int \delta(f-h_a)\frac{G(f)}{E(f)}\,df + \frac{5}{f_m}\left(\frac{h_a}{f_m}\right)^{-4}\phi_1'(G(f)) - \frac{1}{\alpha}\phi_2'(G(f)) - \frac{e^{-0.5}}{\gamma}\phi_3'(G(f))\right)\right] \qquad f < f_m \qquad \text{(A14)}$$

$$\phi_5'(G(f)) = -\frac{1}{f_m}\left[\frac{h_b}{f_m}\phi_1'(G(f)) + \frac{1}{g'(h_b)}\left(\int \delta(f-h_b)\frac{G(f)}{E(f)}\,df + \frac{5}{f_m}\left(\frac{h_b}{f_m}\right)^{-4}\phi_1'(G(f)) - \frac{1}{\alpha}\phi_2'(G(f)) - \frac{e^{-0.5}}{\gamma}\phi_3'(G(f))\right)\right] \qquad f > f_m \qquad \text{(A15)}$$

h_a, h_b are given in (A7).

APPENDIX B. CALCULATION OF D_{ijk} IN THE PARAMETERIZED TRANSPORT EQUATION

The basic method is discussed in I. It is shown there that

$$D_{ijk} = \phi_i'\left(V_k\frac{\partial E}{\partial a_j}\right) \qquad \text{(B1)}$$

where V_k is the k component of group velocity V which in deep water has a magnitude of $g/4\pi f$. To simplify, assume that the x axis lies in the V direction and therefore that D_{ijk} vanishes for $k = 2$. The calculated values of $D_{ijl} \equiv D_{ij}$ according to (B1) are given in Table B1.

For certain parameter regions the parametrized spectrum becomes insensitive to small changes of the parameters. Thus, inversely, the derivatives of the functionals ϕ_i given in Appendix A become very large with respect to these parameters and lead to singularities in the coupling coefficients D_{ij}. This occurs for

$$\begin{aligned} &D_{4,j};\ j = 1, 2, 3, 4 \qquad a_4 \to 1 \\ &D_{i,j};\ i = 4, 5 \qquad j = 1, 2, 3 \qquad a_3 \to 1 \end{aligned} \qquad \text{(B2)}$$

The value of a_4 in (B2) corresponds to an unrealistic wind-sea spectrum. However, the numerical model may produce, locally, parameter values near the values given in the first case of (B2) for special wind fields (jumps in the source function).

Because of this possibility the D_{ij} are modified in the region of the singular points to stabilize the numerical procedure and enable the model to return to realistic parameter values. The modified D_{ij} are given in Table B2.

The second case of (B2) is associated with spectra at or near the fully developed wind-sea state. From (3) we see that the spectrum becomes insensitive to the magnitude of $a_4 = \sigma_a$, $a_5 = \sigma_b$ for $a_3 \to 1$. Therefore it is unimportant that the prognostic equations for a_4, a_5 become singular then. However, to avoid large numbers in the computer runs we change the coefficients D_{4i}, D_{5i} in Table B2 to the coefficients D_{4i}^*, D_{5i}^*, $i = 1, 2, 3$:

$$\begin{aligned} D_{\mu i}^* &= D_{\mu i}^*(a_1, \cdots, a_5) = D_{\mu i}(a_1, \cdots, a_5) \qquad a_3 \geq 2 \\ D_{\mu i}^* &= D_{\mu i}^*(a_1, \cdots, a_5) \\ &= (\gamma - 1)D_{\mu i}(a_1, a_2, a_3 = 2, a_4, a_5) \qquad a_3 \leq 2 \end{aligned} \qquad \text{(B3)}$$

REFERENCES

Barnett, T. P., and J. C. Wilkerson, On the generation of wind waves as inferred from airborne radar measurements of fetch limited spectra, *J. Mar. Res., 25,* 292–328, 1967.

Barnett, T. P., On the generation dissipation and prediction of ocean wind waves, *J. Geophys. Res., 73,* 513–530, 1968.

Barnett, T. P., C. H. Holland, and P. Yager, A general technique for wind-wave prediction with application to the South China Sea, report, Westinghouse Ocean Res. Lab., San Diego, Calif. 1969.

Ewing, J. A., A numerical wave prediction method for the North Atlantic Ocean, *Deut. Hydrogr. Z, 24,* 241–261, 1971.

Ewing, J. A., T. J. Weare, and B. A. Worthington, A hindcast study of extreme wave conditions in the North Sea, *J. Geophys. Res.,* this issue, 1979.

Gelci, R., H. Cazalé, and J. Vassal, Prévision de la houle, La méthode des densités spectroangularies, *Bull. Inform. Comité Central Oceanogr. d'Etude Côtes, 9,* 416, 1957.

Günther, H., W. Rosenthal, Das Problem der Windsee bei der numerischen Vorhersage in der Nordsee, Berichte aus dem Sonderforschungsbereich Meeresforschung, SFB 94, Univ. Hamburg, vol. 10, 52, 1976.

Harding, J., and A. A. Binding, The specification of wind and pressure fields over the North Sea and some areas of the North Atlantic during 42 gales from the period 1966 to 1976, *Rep. 55,* Inst. of Oceanogr. Sci., Wormley, England, 1978.

Hasselmann, K., On the non-linear energy transfer in a gravity-wave spectrum, 1. General theory, *J. Fluid Mech., 12,* 481–500, 1962.

Hasselmann, K., On the non-linear energy transfer in a gravity-wave spectrum, 3, Evaluation of the energy flux and swell-sea interaction for a Neumann spectrum, *J. Fluid Mech., 15,* 385–398, 1963.

Hasselmann, K., T. P. Barnett, E. Bouws, H. Carlson, D. E. Cartwright, K. Enke, J. A. Wieng, H. Gienapp, D. E. Hasselmann, P. Krusemann, A. Meerburg, P. Müller, D. J. Olbers, K. Richter, W. Sell, and H. Walden, Measurements of wind-wave growth and swell decay during the Joint North Sea Wave Project (Jonswap), *Deutsch. Hydrogr. Z.,* suppl. A., *8*(12) 1973.

Hasselmann, K., D. B. Ross, P. Müller, and W. Sell, A parametrical wave prediction model, *J. Phys. Oceanogr., 6,* 201–228, 1976.

Hydraulics Research Station, Numerical wave climate study for the North Sea (Norswam), *Rep. EX775,* Wallingford, England, 1977*a*.

Hydraulics Research Station, Numerical wave climate study for the North Sea, User Manual, *Rep. EX776,* Wallingford, England, 1977*b*.

Inoue, T., On the growth of the spectrum of a wind generated sea according to a modified Miles-Phillips mechanism and its application to wave forecasting, *Rep. TR 67-5,* Geophys. Sci. Lab., New York Univ., 1967.

Kinsman, B. *Wind Waves: Their Generation and Propagation on the Ocean Surface,* 676 pp., Prentice-Hall, Englewood Cliffs, N. J., 1965.

Miles, J. W., On the generation of surface waves by shear flow, 1, *J. Fluid Mech., 3,* 185–204, 1957.

Müller, P., Parametrization of one-dimensional wind wave spectra and their dependence on the state of development, edited by Geophysikalische Institut University of Hamburg, Hamburger Geophysikalische Einzelschriften, 1976.

Phillips, O. M., On the generation of waves by turbulent wind, *J. Fluid Mech., 2,* 417–445, 1957.

Phillips, O. M., On the dynamics of unsteady gravity waves of small amplitude, I, *J. Fluid Mech., 9,* 193–217, 1960.

Phillips, O. M., *The Dynamics of the Upper Ocean,* 261 pp., Cambridge University Press, Oxford, 1966.

Pierson, W. J., Comments on A parametrical wave prediction model, *J. Phys. Oceanogr., 7,* 127–134, 1977.

Pierson, W. J., and L. Moskowitz, A proposed form for fully developed wind seas based on the similarity theory of S. A. Kitagorodskii, *J. Geophys. Res., 69,* 5181–5190, 1964.

Pierson, W. J., L. J. Tick, and L. Baer, Computer based procedures for preparing global wave forecasts and wind field analyses capable of using wave data obtained by a spacecraft, in *Proceedings of the Sixth*

Naval Hydrodynamics Symposium, 499 pp., Office of Naval Research, Washington, D. C., 1966.

Sell, W., and K. Hasselmann, Computations of non-linear energy transfer for Jonswap and empirical wind wave spectra, Inst. Geophys., Univ. of Hamburg, 1972.

Snyder, R. L., A field study of wave-induced pressure fluctuations above surface gravity waves, *J. Mar. Res.*, *32*, 497–531, 1974.

Snyder, R. L., and C. S. Cox, A field study of the wind generation of ocean waves, *J. Mar. Res.*, *24*, 141–178, 1966.

(Received April 13, 1978;
revised August 16, 1978;
accepted August 24, 1978.)